Geophysical Research Letters

Key Points:
- Experimental results indicate CH_4 clumped isotopes are controlled by rates of microbial CH_4 production
- Paired clumped isotopes and ^{14}C measurements imply CH_4 formed from older substrates in northern lakes is produced relatively slowly
- Comparison of clumped isotope data and flux estimates suggests that CH_4 production rate is not a strong determinant of CH_4 ebullition flux

Supporting Information:
- Supporting Information S1
- Table S1

Correspondence to:
P. M. J. Douglas,
peter.douglas@mcgill.ca

Clumped Isotopes Link Older Carbon Substrates With Slower Rates of Methanogenesis in Northern Lakes

Peter M. J. Douglas[1,2] (iD), Regina Gonzalez Moguel[1], Katey M. Walter Anthony[3], Martin Wik[4] (iD), Patrick M. Crill[4] (iD), Katherine S. Dawson[2,5] (iD), Derek A. Smith[2,6], Ella Yanay[2,7], Max K. Lloyd[2,8], Daniel A. Stolper[8], John M. Eiler[2], and Alex L. Sessions[2] (iD)

[1]Department of Earth and Planetary Sciences, McGill University, Montreal, QC, Canada, [2]Division of Geological and Planetary Sciences, California Institute of Technology, Pasadena, CA, USA, [3]International Arctic Research Center, University of Alaska-Fairbanks, Fairbanks, AK, USA, [4]Department of Geological Sciences and Bolin Centre for Climate Research, Stockholm University, Stockholm, Sweden, [5]Department of Environmental Sciences, Rutgers University, New Brunswick, NJ, USA, [6]Department of Biology, Case Western Reserve University, Cleveland, OH, USA, [7]Department of Genetics, Institute of Life Sciences, Hebrew University of Jerusalem, Israel, [8]Department of Earth and Planetary Science, University of California, Berkeley, CA, USA

Abstract The release of long-stored carbon from thawed permafrost could fuel increased methanogenesis in northern lakes, but it remains unclear whether old carbon substrates released from permafrost are metabolized as rapidly by methanogenic microbial communities as recently produced organic carbon. Here, we apply methane (CH_4) clumped isotope (Δ_{18}) and ^{14}C measurements to test whether rates of methanogenesis are related to carbon substrate age. Results from culture experiments indicate that Δ_{18} values are negatively correlated with CH_4 production rate. Measurements of ebullition samples from thermokarst lakes in Alaska and glacial lakes in Sweden indicate strong negative correlations between CH_4 Δ_{18} and the fraction modern carbon. These correlations imply that CH_4 derived from older carbon substrates is produced relatively slowly. Relative rates of methanogenesis, as inferred from Δ_{18} values, are not positively correlated with CH_4 flux estimates, highlighting the likely importance of environmental variables other than CH_4 production rates in controlling ebullition fluxes.

Plain Language Summary There is concern that carbon from thawed permafrost will be emitted to the atmosphere as methane (CH_4). It is currently uncertain whether old organic carbon from thawed permafrost can be converted to CH_4 as rapidly as organic carbon recently fixed by primary producers. We address this question by combining radiocarbon and clumped isotope measurements of CH_4 from lakes in permafrost landscapes. Radiocarbon (^{14}C) measurements indicate the age of CH_4 carbon sources. We present data from culture experiments that support the hypothesis that clumped isotope values are dependent on microbial CH_4 production rate. In lake bubble samples, we observe a strong correlation between these two measurements, which implies that CH_4 formed from older carbon is produced relatively slowly. We also find that higher rates of CH_4 production, as inferred from clumped isotopes, are not linked to higher rates of CH_4 emissions, implying that variables other than CH_4 production rate strongly influence emission rates.

1. Introduction

Thawing of permafrost provides previously frozen organic carbon to anaerobic microbial communities whose respiration releases CO_2 and CH_4. The release of these greenhouse gases constitutes a positive feedback to global warming, with a potential contribution of 174 Pg of carbon to the atmosphere by 2100 (Koven et al., 2011; Schuur et al., 2015). Specific attention has been directed to the potential for lakes in permafrost regions to act as CH_4 emissions sources (Walter Anthony et al., 2018; Wik et al., 2016). Much of this CH_4 could be derived from carbon reservoirs that have been frozen and unavailable for microbial respiration for thousands of years (Walter Anthony et al., 2016), which represents a net input of carbon into the active Earth surface carbon cycle (Archer et al., 2009). ^{14}C measurements of CH_4 are an excellent tracer for the age of carbon sources for methanogenesis. However, ^{14}C measurements of CH_4 in northern lakes span a large range (modern to >50,000 years old) (Bouchard et al., 2015; Elder et al., 2018; Walter et al., 2008), and our understanding of the mechanisms that control this variability remains limited.

If old organic carbon released from permafrost is less reactive than recently fixed carbon, this may limit microbial metabolisms fueled by older carbon, including methanogenesis. This premise is based on the observation that in sediments and soils, older organic carbon is generally less reactive with respect to microbial degradation (Middelburg, 1989; Trumbore, 2000). Recent studies have found, however, that ^{14}C-depleted organic carbon from permafrost can be highly reactive (Ewing et al., 2015; Heslop et al., 2019; Mann et al., 2015; Vonk et al., 2013).

CH_4 stable isotope measurements have the potential to identify differences in CH_4 production rates and how they relate to carbon substrate age. In particular, measurements of multiply substituted isotopologues, or clumped isotopes (Ono et al., 2014; Stolper, Sessions, et al., 2014; Young et al., 2017), in microbial CH_4 are hypothesized to be controlled by the enzymatic reversibility of CH_4 production (Gruen et al., 2018; Stolper et al., 2015; Wang et al., 2015). Enzymatic reversibility of methanogenesis is a function of the forward and reverse reaction rates of methanogenesis (Stolper et al., 2015) and is therefore directly related to the net rate of CH_4 production.

In this study, we combined analyses of clumped isotopes (Δ_{18}; see definition in Section 2) and ^{14}C in samples of CH_4 emitted in bubbles from eight lakes associated with permafrost in Alaska and Sweden to test whether there is a linkage between relative rates of microbial methanogenesis and the age of carbon substrates. The five lakes from Alaska are thermokarst lakes formed by the thaw of ice-rich permafrost (Douglas et al., 2016; Elder et al., 2019; Walter et al., 2008), while the three Swedish lakes are postglacial lakes surrounded by thawing discontinuous permafrost (Wik et al., 2013). To support this analysis, we also present a compilation of new and published Δ_{18} and $\Delta^{13}CH_3D$ measurements from culture experiments to provide empirical evidence that clumped isotope values are related to CH_4 production rate. Finally, we compare Δ_{18} and ^{14}C measurements with CH_4 ebullition flux estimates to inform conceptual models of how CH_4 production rate relates to lake ebullition fluxes.

2. Methods

2.1. Lake Ebullition Sampling

Ebullition gas samples from the Alaskan lakes (Qalluruq, Cake Eater, Goldstream, Doughnut, and Smith) were collected from submerged, umbrella-style bubble traps, following methods described by Walter et al. (2008), between 2009 and 2013. Bubble traps were fixed in place over identified bubble seeps. Ebullition gas samples from the Stordalen lakes (Inre Harrsjön, Mellersta Harrsjön, and Villasjön) were collected using submerged inverted funnels, as described by Wik et al. (2013), in 2013 and 2014. The Stordalen traps were distributed evenly across the lakes since no coherent bubble seeps were identified. Lake locations and classifications are described in more detail in previous studies (Douglas et al., 2016; Walter et al., 2008; Wik et al., 2013).

2.2. Pure Culture Experiments

Pure cultures of *Methanosarcina acetivorans* (Sowers et al., 1984) (Strain DSM 2834; DSMZ GmbH) were grown on a carbon substrate of methanol (MeOH) or trimethylamine (TMA). Cultures in Batch 1 and Batch 2 (Table S1 in the supporting information) were grown in 1 L glass vials in 350 mL of sterile media, while cultures for Batch 3 were grown in 40 mL glass vials in 20 mL of sterile media (Text S1). All cultures were grown under a headspace of N_2 gas at a pressure of 150 kPa. Batch 1 and 2 cultures included 5 mL of either 99.9% MeOH or TMA as a carbon substrate, while Batch 3 cultures included 0.25 mL of 99.9% MeOH (Table S2). The culture bottles were kept in an incubator at 28°C and shaken at 35 rpm. Headspace CH_4 concentrations were either measured prior to sampling for isotopic analysis using an Agilent HP 5890GC-5972MSD (gas chromatograph-mass selective detector; Batch 2) or were measured manometrically during CH_4 preparation for isotopic analysis (Batches 1 and 3). Immediately following CH_4 concentration measurements, aliquots of headspace gas were sampled using a 5 mL gas tight syringe for isotope measurements (see Section 2.6). Culture incubation times are listed in Table S2.

2.3. Enrichment Culture Experiments

Enrichment cultures were established using sediments from two aquatic environments in Southern California: Baxter Pond, an artificial pond on the Caltech campus (Stolper et al., 2015); and the Ballona

wetlands, a coastal marsh. Cultures were grown in a headspace of 80:20 H_2:CO_2, in a sterile media (Text S1), with 180 µL of 1 M sodium acetate. The cultures were transferred every 5 days, with an additional 180 µL of 1 M sodium acetate added at each transfer. Twenty days after the fifth transfer, the cultures were analyzed for headspace CH_4 concentrations using an Agilent HP 5890GC-5972MSD and sampled for isotopic analysis.

2.4. Estimation of CH_4 Production Rates in Culture Experiments

We estimated the net CH_4 production rate (r_{net}; mg CH_4 hr^{-1} ml media^{-1}) using the following equation:

$$r_{net} = \frac{f_{CH4} V_{HS} P M_{CH4}}{RTt V_m},$$

(1)

where f_{CH4} is the fractional concentration of CH_4 in the culture headspace, V_{HS} is the volume of the headspace (in L), P is the headspace pressure (kPa), M_{CH4} is the molar mass of CH_4 (mg mol^{-1}), R is the ideal gas constant, T is temperature (K), t is the time from culture inoculation to sampling (hours), and V_m is the volume of the culture media (ml). CH_4 production rates for experiments performed at MIT were calculated from data reported by Gruen et al. (2018).

2.5. CH_4 Radiocarbon Measurements

CH_4 $^{14}C/^{12}C$ ratios for the Alaskan lake samples were measured at the National Ocean Sciences Accelerator Mass Spectrometry facility, as described by Brosius et al. (2012) and Walter Anthony et al. (2012). $^{14}C/^{12}C$ analysis for the samples from Stordalen mire was analyzed at the A.E. Lalonde Accelerator Mass Spectrometry Laboratory (University of Ottawa), using a preparation procedure based on that of Pack et al. (2015). Radiocarbon data are expressed in fraction modern (Fm) as defined by Stuiver and Polach (1977). Blank tests were conducted alongside all sample ^{14}C analyses, and no evidence for significant blank carbon was found.

2.6. Clumped Isotope and Other Stable Isotope Measurements

CH_4 was purified from mixed gas samples using a vacuum line cryotrapping method described previously (Douglas et al., 2016; Stolper, Lawson, et al., 2014; Stolper, Sessions, et al., 2014), resulting in CH_4 purity of ~99.9%.

CH_4 δD, $δ^{13}C$, and $Δ_{18}$ for all samples, except the Batch 3 pure culture experiments, were measured using a prototype Thermo 253 Ultra (Eiler et al., 2013) at Caltech, as described in detail previously (Stolper, Sessions, et al., 2014). The Batch 3 pure culture experiments were analyzed for CH_4 δD, $δ^{13}C$, and $Δ^{13}CH_3D$ and for three samples $Δ^{12}CH_2D_2$, using a production model Thermo 253 Ultra at the University of California, Berkeley, as described by Eldridge et al. (2019). δD and $δ^{13}C$ values are expressed using delta notation relative to Vienna Standard Mean Ocean Water and Vienna Pee Dee Belemnite, respectively.

Most (90%) of the clumped isotope compositions presented here are expressed using $Δ_{18}$ notation as described by Stolper, Sessions, et al. (2014), where

$$Δ_{18} = \left(^{18}R/^{18}R^* - 1\right),$$

(2)

and

$$^{18}R = \left(\left[^{13}CH_3D\right] + \left[^{12}CH_2D_2\right]\right)/\left[^{12}CH_4\right].$$

(3)

$^{18}R^*$ is the ^{18}R value expected for a random internal distribution of isotopologues, given the $δ^{13}C$ and δD values of the sample (Stolper, Sessions, et al., 2014) and is expressed as

$$^{18}R^* = \left(6 \times \left[^2R\right]^2\right) + \left(4 \times {}^2R \times {}^{13}R\right).$$

(4)

$Δ_{18}$ data are reported as per mil (‰), where 0‰ refers to a random distribution of CH_4 isotopologues (i.e., $^{18}R = {}^{18}R^*$). All samples are referenced against a laboratory standard with a $Δ_{18}$ value of 2.981 ± 0.015‰ (Stolper, Sessions, et al., 2014). External reproducibility for $Δ_{18}$, δD, and $δ^{13}C$ values (1σ) was 0.38 ‰, 0.22 ‰, and 0.06 ‰ respectively.

CH_4 samples from the Batch 3 culture experiments were measured for δD, $\delta^{13}C$, and $\Delta^{13}CH_3D$ and for three samples $\Delta^{12}CH_2D_2$. A complete description of the analytical methods used for this measurement is found in Eldridge et al. (2019). The equations for these measurements (corresponding to Equations 2–4), and details on standards and reproducibility are listed in the Text S1. Where both $\Delta^{13}CH_3D$ and Δ_{18} measurements are discussed together we use the term Δ_{18}, as this is the more general term (Stolper, Sessions, et al., 2014).

$\delta^{13}C$ of CO_2 from the Alaskan gas samples were measured at Florida State University, as described by Walter Anthony et al. (2012).

2.7. Gas Concentration and Flux Measurements

The concentrations of CH_4 and other gases in the Alaskan lake samples were measured at the University of Alaska-Fairbanks, as described in Walter Anthony et al. (2012). For most Alaskan samples, bubble gas fluxes are estimated using the average flux measurements of seeps from a given seep classification (Lindgren et al., 2016; Walter Anthony & Anthony, 2013) (Table S1). In the Alaskan data set, all samples were collected from identified point source seeps, and flux estimates were not dependent on the area of the traps.

CH_4 concentrations in the Stordalen lake samples were measured at the Abisko Scientific Research Station as described by Wik et al. (2013). Gas fluxes were estimated by measuring gas volume accumulations in bubble traps manually. To account for scaling effects related to the area of the traps, for these samples, we report flux in terms of L CH_4 day^{-1} m^{-2} (Table S1). In one case where a sample-specific flux was not available, we adopted the 6-year average flux for that trap. In all samples, CH_4 flux was calculated by multiplying the estimated gas flux by the measured CH_4 concentration.

2.8. Model of CH_4 Kinetic Isotope Effects

Predicted CH_4 kinetic isotope effects are based on the model of Stolper et al. (2015), with modifications of two model parameters. First, we reduced $\kappa_{f\text{-}}{}^{13}CH_3D$ (the ratio of rate constants that describe the relative rate of formation of two isotopologues from a methyl precursor for $^{13}CH_3D/^{12}CH_4$) from 1.935 to 1.934 to account for low Δ_{18} and Δ_{13CH3D} values ($\sim{-}5‰$) observed in some culture experiments. Second, we reduced $\kappa_f\text{-}{}^{12}CH_2D_2$ (as above but for $^{12}CH_2D_2/^{12}CH_4$) from 1.89 to 1.63 to account for measurements of $\Delta^{13}CH_3D$ and $\Delta^{12}CH_2D_2$ in CH_4 from pure culture experiments (Young et al., 2017) that indicate negative $\Delta^{12}CH_2D_2$ corresponding to negative $\Delta^{13}CH_3D$ values.

The kinetic isotope effect model relates CH_4 isotopologue ratios to the degree of reversibility of CH_4 generation (ρ). In order to relate modeled Δ_{18} and Δ_{13CH3D} values to net CH_4 production rates (r_{net}), we used the following equation from Stolper et al. (2015):

$$\rho = \frac{^{12_{CH_4}}k_{rev}}{^{12_{CH_4}}k_{rev} + {}^{12_{CH_4}}k_{net}} \tag{5}$$

where k_{rev} and k_{net} are the first-order rate constants of reverse methanogenesis and net extracellular $^{12}CH_4$ production, respectively. These reaction constants are related to the net (r_{net}) and reverse (r_{rev}) reaction rates of methanogenesis by the following relationships:

$$r_{net} = k_{net}[CH_4], \tag{6}$$

$$r_{rev} = k_{rev}[CH_4], \tag{7}$$

where $[CH_4]$ is the intracellular concentration of CH_4.

Combining Equations 5–7, it follows that

$$r_{net} = \frac{r_{rev}}{\rho} - r_{rev}. \tag{8}$$

To compare the modeled relationship between $\Delta_{18}/\Delta^{13}CH_3D$ values and r_{net} with empirical estimates of CH_4 production rates from culture experiments, we made three assumptions. First, we assumed a constant value for r_{rev} (Timmers et al., 2017; Vavilin, 2013; Vavilin & Rytov, 2013), specifically 4×10^{-4} mg CH_4 hr^{-1} ml^{-1}. This value was chosen because it produces the best fit, as defined by the lowest root mean square error
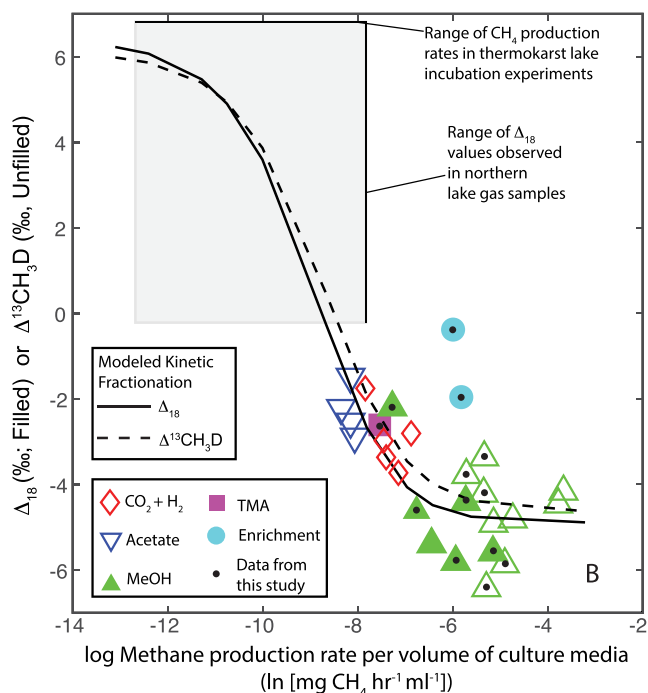
Figure 1. Plot of the natural log of CH_4 production rate (r_{net}) vs. Δ_{18} or $\Delta^{13}CH_3D$ in pure and enrichment culture experiments. Data are from Douglas et al. (2016), Gruen et al. (2018), and this study (new data indicated by black dots). Solid and dashed lines indicate predicted values based on a model of methanogenesis kinetic isotope effects (Stolper et al., 2015) (Section 2.8). The gray rectangle indicates the empirical ranges of these two variables observed in Alaskan thermokarst lakes, specifically the Δ_{18} values of ebullition gas samples (this study), and CH_4 production rates of incubated thermokarst lake sediments and thawed permafrost (Heslop et al., 2015). Analytical errors for Δ_{18} or $\Delta^{13}CH_3D$ measurements (1σ) are smaller than the symbols. MeOH, methanol; TMA, trimethylamine.

(RMSE = 0.87‰), between observed and predicted Δ_{13CH3D} and Δ_{18} values. Second, the model describes cell-specific values for r_{rev} and r_{net}, but we did not measure cell density for the pure and enrichment culture experiments. This means that when comparing to the empirical results, the assumed value of r_{rev} and modeled values of r_{net} are instead expressed per volume of culture media. Third, the model was specifically developed for hydrogenotrophic methanogenesis (Stolper et al., 2015), but we are comparing it to CH_4 produced using four different substrates. See Text S1 for a detailed rationale for these assumptions.

3. Results and Discussion

3.1. Clumped Isotope Values in Culture Experiments Reflect CH_4 Production Rates

CH_4 sampled from freshwater ecosystems and from methanogen culture experiments exhibits low or negative Δ_{18} values that indicate strong kinetic isotope effects (Douglas et al., 2016; Giunta et al., 2019; Gruen et al., 2018; Stolper et al., 2015; Wang et al., 2015; Young et al., 2017). Isotopic models of hydrogenotrophic methanogenesis predict that this kinetic isotope effect is controlled by the reversibility of the enzymatic reactions of methanogenesis (Stolper et al., 2015; Valentine et al., 2004; Wang et al., 2015). In pure culture experiments where CH_4 production rate was measured, using four different carbon substrates, there is a non-linear negative relationship between CH_4 production rate and Δ_{18} (Figure 1). This finding supports the hypothesis that Δ_{18} in microbial CH_4 varies as a function of the rate of methanogenesis.

Assuming a constant value for r_{rev} (see Section 2.8), the relationship between r_{net} and Δ_{18} predicted by a model of kinetic isotope effects (Stolper et al., 2015) provides a good fit to the shape of the empirical relationship seen in the pure culture experiments. The two enrichment cultures derived from wetland sediments indicate higher Δ_{18} values for a given CH_4 production rate than the pure culture experiments, possibly as a result of higher values of r_{rev} or the occurrence of anaerobic CH_4 oxidation (Figure S1). The modeled relationship between r_{net} and Δ_{18} from the pure cultures spans a plausible range of values for northern lakes, based on CH_4 production rates from incubation experiments of thermokarst lake sediments (Heslop et al., 2015) (Figure 1). Although there is uncertainty in quantitatively relating Δ_{18} to CH_4 production rates in environmental samples, we propose that Δ_{18} values can be used as an indicator of relative differences in CH_4 production rates between samples.

3.2. Linkages Between Carbon Substrate Age and Rates of Methanogenesis

There is a significant positive correlation ($p < 0.05$) between Δ_{18} and Fm for both the Alaskan and Stordalen lakes (Figure 2), although the relationship is offset to higher Fm values in the Stordalen lakes. Based on our working hypothesis described above, the observed correlations imply that the rate of methanogenesis within these environments is lower when CH_4-producing microbial communities metabolize older carbon substrates.

Other biogeochemical variables, including variation in methanogenic pathways, methane oxidation, and substrate depletion could also potentially influence Δ_{18} values in these environments, although the effects of these variables on Δ_{18} are not well defined (Ash et al., 2019; Giunta et al., 2019; Gruen et al., 2018; Wang et al., 2016; Young et al., 2017). However, the relationship between Δ_{18} and CH_4 production rate in pure culture experiments appears to be consistent across different methanogenic pathways (Figure 1). Furthermore, the absence of a significant correlation between CH_4 Fm and $\delta^{13}C$ values in these samples (Figure S4) implies that variation in methane oxidation or substrate depletion is probably not controlling the observed relationship between Δ_{18} and Fm (Hayes, 2001; Whiticar, 1999). Lake Qalluruq on the north
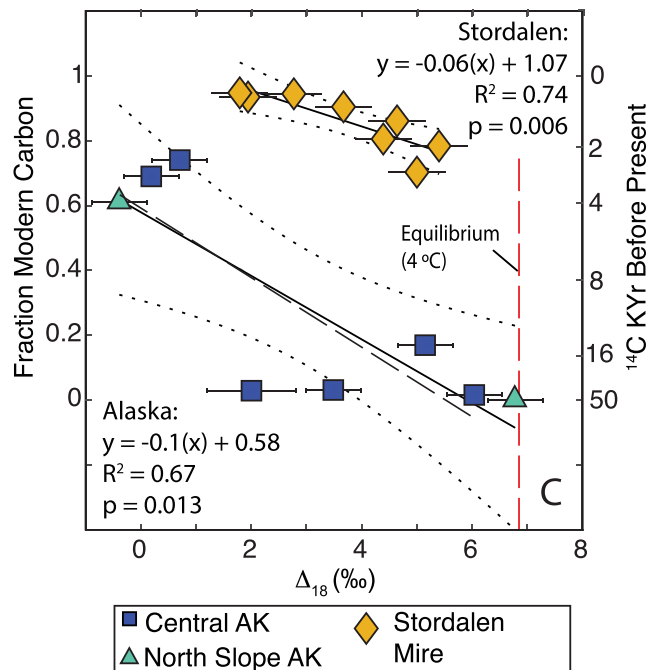
Figure 2. Plot of Δ_{18} vs. Fm for both sets of CH$_4$ samples. The dashed red line indicates the equilibrium Δ_{18} value at 4°C. Dotted lines indicate the 95% confidence interval for linear regression fits. The dashed black line indicates the Alaskan regression fit excluding Lake Qalluruq ($y = -0.11x + 0.59$; $R^2 = 0.64$; $p = 0.03$). Horizontal error bars indicate the analytical error (2σ) for Δ_{18} measurements. Analytical errors for Fm values are smaller than the symbols.

slope of Alaska may be anomalous because isotopic and gas composition data imply its CH$_4$ emissions are derived from microbial methanogenesis in subpermafrost coal deposits that underlie the lake (Douglas et al., 2016; Walter Anthony et al., 2012). If this lake is excluded, we still observe a significant relationship between Δ_{18} and Fm for the Alaskan samples (Figure 2).

A plausible mechanism linking Δ_{18} values and Fm is that older carbon reservoirs have undergone a greater degree of microbial decomposition (Middelburg, 1989; Trumbore, 2000) and therefore contain a greater proportion of recalcitrant organic molecules that limit microbial metabolisms. The range of Δ_{18} values in the Alaskan and Stordalen samples overlaps, implying a similar range of CH$_4$ production rates in these ecosystems despite the large difference in carbon substrate ages. The mean age of organic carbon in the Stordalen lake catchments is significantly younger than that in the Alaskan lakes, largely due to the Stordalen lakes catchments history of Holocene deglaciation (Walter Anthony et al., 2016). Differences in organic matter reactivity could explain the different Δ_{18}-Fm relationships between the Alaskan and Stordalen sample sets. In the Alaskan thermokarst lakes, old organic matter has largely been stored frozen and was therefore subject to limited decomposition and could remain relatively reactive (Ewing et al., 2015). In contrast, the organic matter in the Stordalen lake sediments is not predominantly derived from thawed permafrost (Kokfelt et al., 2010) and therefore is more likely to become increasingly refractory with time. The reactivity of organic carbon is also likely influenced by active layer dynamics prior to freezing. For example, yedoma is composed of eolian deposits (Schuur et al., 2015) and undergoes different soil formation processes than other terrestrial permafrost.

It is noteworthy that organic matter in thawed permafrost has been shown to be highly available for microbial degradation regardless of its ^{14}C age (Ewing et al., 2015; Mann et al., 2015; Vonk et al., 2013). In addition, deep yedoma permafrost (>12 m depth) from Central Alaska contains a high proportion of labile organic compounds (reduced and saturated OC compounds), and in laboratory incubations produces CH$_4$ more rapidly than shallower permafrost or active layer soils (Heslop et al., 2019). We consider reduced reactivity of organic carbon to be the simplest mechanism linking older carbon substrates to slower rates of methanogenesis, but other environmental variables such as the concentration of alternate electron acceptors or temperature could also explain this linkage. Both thawing and intact permafrost often contain relatively high concentrations of iron oxides, nitrate, or sulfate that can be reduced to respire organic carbon, thereby inhibiting methanogenesis. (Herndon et al., 2017; Heslop et al., 2019; Keuper et al., 2012; Winkel et al., 2019). Additionally, rates of methanogenesis have been shown to increase at higher temperatures (Yvon-Durocher et al., 2014). Deep thawed permafrost does not warm substantially in the summer as compared to shallower sediments or soils, and warm summer temperatures could cause higher rates of methanogenesis in shallow lake sediments relative to deeper environments (Wik et al., 2014).

3.3. Relative Rates of Methanogenesis Are Not Positively Related to CH$_4$ Ebullition Flux

In the Alaskan thermokarst lakes, we also observe that Δ_{18} is positively correlated with the logarithm of CH$_4$ flux (Figure 3b). This relationship is counterintuitive, as it implies that CH$_4$ produced more slowly, from older carbon substrates, is released with a higher flux. Our proposed explanation for this result relies on a conceptual model for thermokarst lake ebullition seeps proposed by Walter et al. (2007) (Figure 3a). In this model, small "point-source" seeps release CH$_4$ from relatively young lake sediments. In contrast, large "hotspot" seeps release CH$_4$ from old thawed permafrost that is concentrated along preferential flow pathways at depth before being emitted near the active thermokarst erosion zone. The Δ_{18} data set implies that point-source seeps are fed by relatively rapid production of CH$_4$ but are limited in the volume of sediment across which they integrate gas, resulting in relatively low CH$_4$ fluxes. Conversely, hotspot seeps are
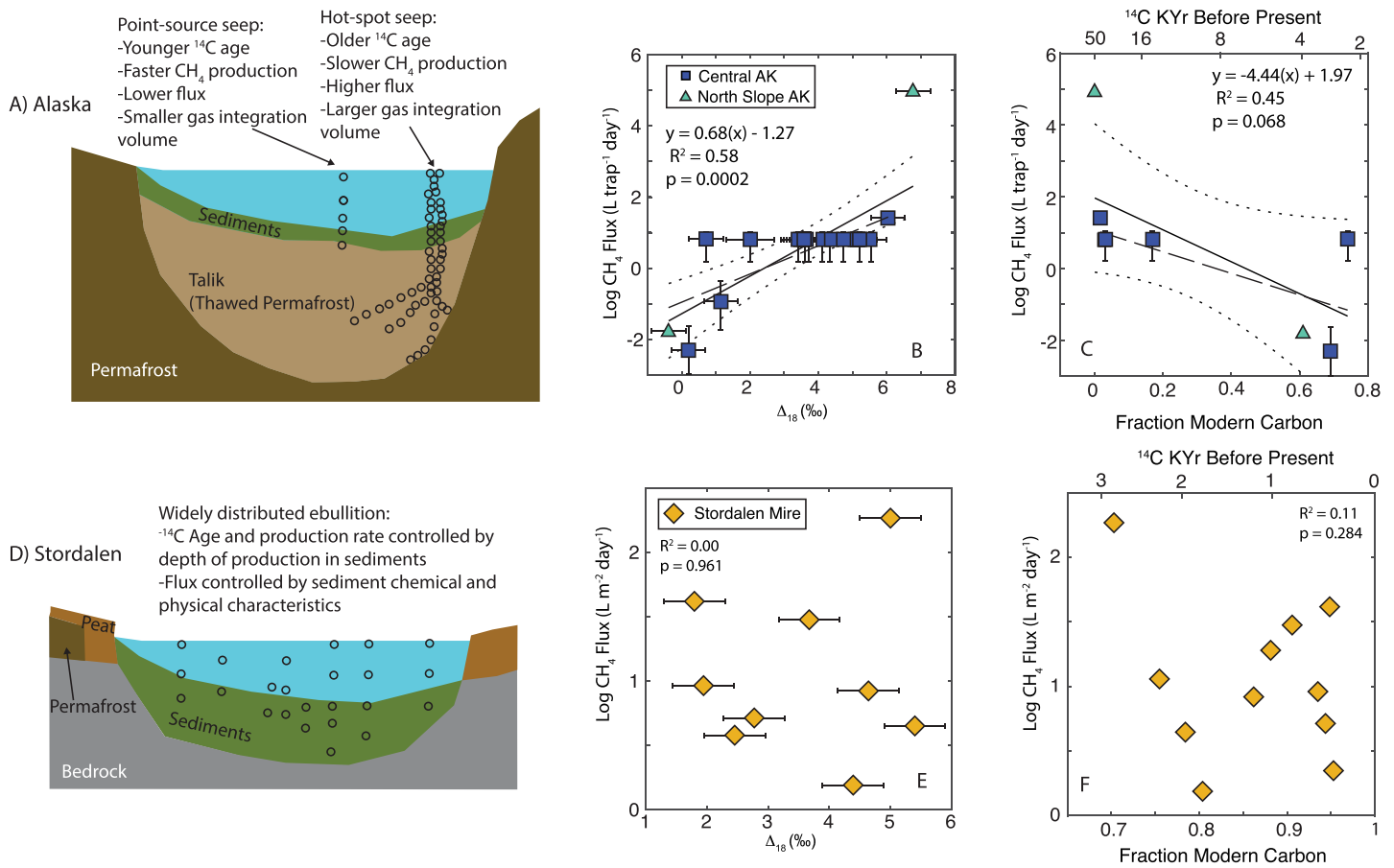
Figure 3. (a) Conceptual model of CH_4 ebullition fluxes in the Alaskan thermokarst lakes; (b) plot of CH_4 flux vs. Δ_{18} for the Alaskan lakes. Dashed black line: regression fit excluding Lake Qalluruq ($y = 0.39x - 0.95$; $R^2 = 0.66$; $p < 0.01$). (c) Plot of CH_4 flux vs. Fm for the Alaskan lakes. Dashed black line: regression fit excluding Lake Qalluruq ($y = -3x + 1.07$; $R^2 = 0.47$; $p = 0.09$). Dotted lines in (b) and (c) indicate 95% confidence intervals for regression fits. Error bars in (b) and (c) indicate standard deviations for average fluxes for different seep types (Walter Anthony & Anthony, 2013). (d) Conceptual model of CH_4 ebullition fluxes in Stordalen glacial lakes; (e) plot of CH_4 flux vs. Δ_{18} for the Stordalen lakes; (f) plot of CH_4 flux vs. Fm for the Stordalen lakes. Horizontal error bars in (b) and (e) indicate analytical error (2σ) for Δ_{18}. Panels (b), (e), and (f) include data that do not have paired ^{14}C and Δ_{18} measurements (Table S1).

fueled by relatively slow production of CH_4 and as such must integrate gas across a much larger volume of thawed permafrost to result in the observed higher CH_4 fluxes. While hotspot seeps occur less frequently than point-source seeps, their large fluxes mean they can emit a large proportion of the total lake ebullition CH_4 flux. At Goldstream Lake, which has been intensively studied in terms of seep densities, hotspot seeps emit 50–70% of total lake ebullition CH_4 fluxes (Walter Anthony & Anthony, 2013).

In contrast, in the Stordalen lakes, we do not observe a significant correlation ($p < 0.05$) between CH_4 ebullition flux and either Δ_{18} (Figure 3e) or Fm (Figure 3f), although there is much less variation in CH_4 flux relative to the Alaskan lakes. This suggests that in the Stordalen lakes variation in CH_4 ebullition flux is not dependent on either the rate of methanogenesis or the age of carbon substrates. We propose that these bubble fluxes are controlled primarily by vertical displacement through low density sediments once gases achieve sufficient pressure in porewaters (Langenegger et al., 2019) and that concentration of gas along preferential flow pathways is minimal. Therefore, while methanogenesis in deeper and older sediments appears to proceed at slower rates (Figure 2), the dominant controls on observed CH_4 ebullition fluxes are likely other physical and chemical variables such as the overall concentration of organic matter and sediment porosity and tortuosity (Ramirez et al., 2015).

The two different models of CH_4 ebullition fluxes discussed above reflect the different sedimentary and geomorphological environments in the Alaskan and Stordalen lakes. The Alaskan thermokarst lakes form in ice-rich permafrost. It is possible that voids produced by melting ice wedges and heterogeneities in thawed permafrost soils enhance the formation of preferential gas flow pathways (Heslop et al., 2015; Rowland et al., 2011; Walter et al., 2008). In contrast, the Stordalen lake basins contain relatively homogenous organic-rich mud overlying bedrock (Kokfelt et al., 2010; Wik et al., 2013), which likely minimizes preferential gas flow pathways. These differences are consistent with studies suggesting that the flux and age of CH_4 emitted from permafrost-associated lakes is influenced by their geological and geomorphological setting (Elder et al., 2018).

This study only considered ebullition fluxes of CH_4, and there are no studies comparing Δ_{18} with ^{14}C or flux for dissolved CH_4. Where comparison is possible, dissolved CH_4 tends to contain younger carbon than ebullition CH_4 (Elder et al., 2019) and is more likely to have its stable isotope composition influenced by methane oxidation (Elder et al., 2019; Jansen et al., 2019). Further study will be needed to assess whether the patterns observed here for ebullition CH_4 also apply to diffusive CH_4 fluxes. However, for the studied lakes, ebullition fluxes are estimated to be the dominant source of CH_4 emissions in the ice-free season (Jansen et al., 2019; Sepulveda-Jauregui et al., 2015).

4. Conclusions

As permafrost thaws, increasing quantities of long-stored carbon will be made available to anaerobic, CH_4-producing microbial communities in lakes. Our data from two different types of northern lakes, supported by results from culture experiments, suggest that methanogenesis using these old carbon substrates will proceed at slower rates than methanogenesis fueled by modern carbon in similar environments. When combined with flux estimates, these results also imply that the inferred relative rates of methanogenesis are not a strong determinant of observed CH_4 ebullition fluxes. More research is needed to constrain the mechanism behind this apparent limitation on the rate of CH_4 production from older carbon, to determine whether these results are representative of other northern lakes and other emissions pathways, and to better understand the relationship between rates of methanogenesis and CH_4 fluxes. If found to be a widespread phenomenon, relatively slow rates of CH_4 production from old carbon substrates could prove to be important in modeling and predicting the emission of CH_4 produced from thawed permafrost.

References

Archer, D., Eby, M., Brovkin, V., Ridgwell, A., Cao, L., Mikolajewicz, U., et al. (2009). Atmospheric lifetime of fossil fuel carbon dioxide. *Annual Review of Earth and Planetary Sciences*, *37*, 117–134.

Ash, J., Egger, M., Treude, T., Kohl, I., Cragg, B., Parkes, R., et al. (2019). Exchange catalysis during anaerobic methanotrophy revealed by $^{12}CH_2D_2$ and $^{13}CH_3D$ in methane. *Geochemical Perspectives Letters*, *10*, 26–30.

Bouchard, F., Laurion, I., Preskienis, V., Fortier, D., Xu, X., & Whiticar, M. (2015). Modern to millennium-old greenhouse gases emitted from ponds and lakes of the Eastern Canadian Arctic (Bylot Island, Nunavut). *Biogeosciences*, *12*, 7279–7298.

Brosius, L., Walter Anthony, K., Grosse, G., Chanton, J., Farquharson, L., Overduin, P. P., & Meyer, H. (2012). Using the deuterium isotope composition of permafrost meltwater to constrain thermokarst lake contributions to atmospheric CH_4 during the last deglaciation. *Journal of Geophysical Research*, *117*, G01022. https://doi.org/10.1029/2011JG001810

Douglas, P., Stolper, D. A., Smith, D. A., Anthony, K. M. W., Paull, C. K., Dallimore, S., et al. (2016). Diverse origins of Arctic and subarctic methane point source emissions identified with multiply-substituted isotopologues. *Geochimica et Cosmochimica Acta*, *188*, 163–188. https://doi.org/10.1016/j.gca.2016.05.031

Eiler, J. M., Clog, M., Magyar, P., Piasecki, A., Sessions, A., Stolper, D., et al. (2013). A high-resolution gas-source isotope ratio mass spectrometer. *International Journal of Mass Spectrometry*, *335*, 45–56.

Elder, C., Xu, X., Walker, J., Schnell, J. L., Hinkel, K. M., Townsend-Small, A., et al. (2018). Greenhouse gas emissions from diverse Arctic Alaskan lakes are dominated by young carbon. *Nature Climate Change*, *8*, 166.

Elder, C. D., Schweiger, M., Lam, B., Crook, E. D., Xu, X., Walker, J., et al. (2019). Seasonal sources of whole-Lake CH_4 and CO_2 emissions from interior Alaskan Thermokarst Lakes. *Journal of Geophysical Research: Biogeosciences*, *124*, 1209–1229. https://doi.org/10.1029/2018JG004735

Eldridge, D. L., Korol, R., Lloyd, M. K., Turner, A. C., Webb, M. A., Miller, T. F., & Stolper, D. (2019). Comparison of experimental vs. theoretical abundances of $^{13}CH_3D$ and $^{12}CH_2D_2$ for isotopically equilibrated systems from 1-500°C. *ACS Earth and Space Chemistry*, *3*, 2747–2764.

Ewing, S. A., O'Donnell, J. A., Aiken, G. R., Butler, K., Butman, D., Windham-Myers, L., & Kanevskiy, M. Z. (2015). Long-term anoxia and release of ancient, labile carbon upon thaw of Pleistocene permafrost. *Geophysical Research Letters*, *42*, 10,730–10,738. https://doi.org/10.1002/2015GL066296

Giunta, T., Young, E. D., Warr, O., Kohl, I., Ash, J. L., Martini, A., et al. (2019). Methane sources and sinks in continental sedimentary systems: New insights from paired clumped isotopologues $^{13}CH_3D$ and $^{12}CH_2D_2$. *Geochimica et Cosmochimica Acta*, *245*, 327–351.

Gruen, D. S., Wang, D. T., Könneke, M., Topçuoğlu, B. D., Stewart, L. C., Goldhammer, T., et al. (2018). Experimental investigation on the controls of clumped isotopologue and hydrogen isotope ratios in microbial methane. *Geochimica et Cosmochimica Acta*, *237*, 339–356.

Hayes, J. M. (2001). Fractionation of carbon and hydrogen isotopes in biosynthetic processes. *Reviews in Mineralogy and Geochemistry*, *43*, 225–277.

Herndon, E., AlBashaireh, A., Singer, D., Chowdhury, T. R., Gu, B., & Graham, D. (2017). Influence of iron redox cycling on organo-mineral associations in Arctic tundra soil. *Geochimica et Cosmochimica Acta*, *207*, 210–231.

Heslop, J., Anthony, W., Katey, M., Sepulveda-Jauregui, A., Martinez-Cruz, K., Bondurant, A., et al. (2015). Thermokarst lake methano-genesis along a complete talik profile. *Biogeosciences*, *12*, 4317–4331.

Heslop, J., Winkel, M., Walter Anthony, K., Spencer, R., Podgorski, D., Zito, P., et al. (2019). Increasing organic carbon biolability with depth in yedoma permafrost: Ramifications for future climate change. *Journal of Geophysical Research: Biogeosciences*, *124*, 2021–2038. https://doi.org/10.1029/2018JG004712

Jansen, J., Thornton, B. F., Jammet, M. M., Wik, M., Cortés, A., Friborg, T., et al. (2019). Climate-sensitive controls on large spring emis-sions of CH_4 and CO_2 from Northern Lakes. *Journal of Geophysical Research: Biogeosciences*, *124*, 2379–2399. https://doi.org/10.1029/2019JG005094

Keuper, F., Van Bodegom, P. M., Dorrepaal, E., Weedon, J. T., Van Hal, J., Van Logtestijn, R. S., & Aerts, R. (2012). A frozen feast: Thawing permafrost increases plant-available nitrogen in subarctic peatlands. *Global Change Biology*, *18*, 1998–2007.

Kokfelt, U., Reuss, N., Struyf, E., Sonesson, M., Rundgren, M., Skog, G., et al. (2010). Wetland development, permafrost history and nutrient cycling inferred from Late Holocene peat and lake sediment records in subarctic Sweden. *Journal of Paleolimnology*, *44*, 327–342.

Koven, C. D., Ringeval, B., Friedlingstein, P., Ciais, P., Cadule, P., Khvorostyanov, D., et al. (2011). Permafrost carbon-climate feedbacks accelerate global warming. *Proceedings of the National Academy of Sciences*, *108*, 14,769–14,774.

Langenegger, T., Vachon, D., Donis, D., & McGinnis, D. (2019). What the bubble knows: Lake methane dynamics revealed by sediment gas bubble composition. *Limnology and Oceanography*, *64*, 1526–1544.

Lindgren, R., Grosse, G., Walter Anthony, K., & Meyer, F. (2016). Detection and spatiotemporal analysis of methane ebullition on ther-mokarst lake ice using high-resolution optical aerial imagery. *Biogeosciences*, *13*, 27–44.

Mann, P. J., Eglinton, T. I., McIntyre, C. P., Zimov, N., Davydova, A., Vonk, J. E., et al. (2015). Utilization of ancient permafrost carbon in headwaters of Arctic fluvial networks. *Nature Communications*, *6*, 7856.

Middelburg, J. J. (1989). A simple rate model for organic matter decomposition in marine sediments. *Geochimica et Cosmochimica Acta*, *53*, 1577–1581.

Ono, S., Wang, D. T., Gruen, D. S., Sherwood Lollar, B., Zahniser, M., McManus, B. J., & Nelson, D. D. (2014). Measurement of a doubly-substituted methane isotopologue, $^{13}CH_3D$, by tunable infrared laser direct absorption spectroscopy. *Analytical Chemistry*, *86*(13), 6487–6494. https://doi.org/10.1021/ac5010579

Pack, M. A., Xu, X., Lupascu, M., Kessler, J. D., & Czimczik, C. I. (2015). A rapid method for preparing low volume CH_4 and CO_2 gas samples for ^{14}C AMS analysis. *Organic Geochemistry*, *78*, 89–98.

Ramirez, J. A., Baird, A. J., Coulthard, T. J., & Waddington, J. M. (2015). Testing a simple model of gas bubble dynamics in porous media. *Water Resources Research*, *51*, 1036–1049. https://doi.org/10.1002/2014WR015898

Rowland, J. C., Travis, B. J., & Wilson, C. (2011). The role of advective heat transport in talik development beneath lakes and ponds in discontinuous permafrost. *Geophysical Research Letters*, *38*, L17504. https://doi.org/10.1029/2011GL048497

Schuur, E., McGuire, A., Schädel, C., Grosse, G., Harden, J. W., Hayes, D. J., et al. (2015). Climate change and the permafrost carbon feedback. *Nature*, *520*(7546), 171–179. https://doi.org/10.1038/nature14338

Sepulveda-Jauregui, A., Walter Anthony, K. M., Martinez-Cruz, K., Greene, S., & Thalasso, F. (2015). Methane and carbon dioxide emis-sions from 40 lakes along a north–south latitudinal transect in Alaska. *Biogeosciences*, *12*, 3197–3223.

Sowers, K. R., Baron, S. F., & Ferry, J. G. (1984). Methanosarcina acetivorans sp. nov., an acetotrophic methane-producing bacterium isolated from marine sediments. *Applied and Environmental Microbiology*, *47*(5), 971–978.

Stolper, D., Lawson, M., Davis, C. L., Ferreira, A. A., Santos Neto, E. V., Ellis, G. S., et al. (2014). Formation temperatures of thermogenic and biogenic methane. *Science*, *344*(6191), 1500–1503. https://doi.org/10.1126/science.1254509

Stolper, D., Martini, A., Clog, M., Douglas, P., Shusta, S., Valentine, D., et al. (2015). Distinguishing and understanding thermogenic and biogenic sources of methane using multiply substituted isotopologues. *Geochimica et Cosmochimica Acta*, *161*, 219–247.

Stolper, D., Sessions, A., Ferreira, A., Santos Neto, E., Schimmelmann, A., Shusta, S., et al. (2014). Combined ^{13}C–D and D–D clumping in methane: Methods and preliminary results. *Geochimica et Cosmochimica Acta*, *126*, 169–191.

Stuiver, M., & Polach, H. A. (1977). Discussion; reporting of ^{14}C data. *Radiocarbon*, *19*, 355–363.

Timmers, P. H., Welte, C. U., Koehorst, J. J., Plugge, C. M., Jetten, M. S., & Stams, A. J. (2017). Reverse methanogenesis and respiration in methanotrophic archaea. *Archaea*, *2017*.

Trumbore, S. (2000). Age of soil organic matter and soil respiration: Radiocarbon constraints on belowground C dynamics. *Ecological Applications*, *10*, 399–411.

Valentine, D. L., Chidthaisong, A., Rice, A., Reeburgh, W. S., & Tyler, S. C. (2004). Carbon and hydrogen isotope fractionation by mod-erately thermophilic methanogens. *Geochimica et Cosmochimica Acta*, *68*, 1571–1590.

Vavilin, V. (2013). Estimating changes of isotopic fractionation based on chemical kinetics and microbial dynamics during anaerobic methane oxidation: Apparent zero-and first-order kinetics at high and low initial methane concentrations. *Antonie Van Leeuwenhoek*, *103*(2), 375–383. https://doi.org/10.1007/s10482-012-9818-8

Vavilin, V., & Rytov, S. (2013). Non-linear dynamics of carbon and hydrogen isotopic signatures based on a biological kinetic model of nitrite-dependent methane oxidation by "Candidatus Methylomirabilis oxyfera". *Antonie Van Leeuwenhoek*, *104*(6), 1097–1108. https://doi.org/10.1007/s10482-013-0031-1

Vonk, J. E., Mann, P. J., Davydov, S., Davydova, A., Spencer, R. G., Schade, J., et al. (2013). High biolability of ancient permafrost carbon upon thaw. *Geophysical Research Letters*, *40*, 2689–2693. https://doi.org/10.1002/grl.50348

Walter Anthony, K., & Anthony, P. (2013). Constraining spatial variability of methane ebullition seeps in thermokarst lakes using point process models. *Journal of Geophysical Research: Biogeosciences*, *118*, 1015–1034. https://doi.org/10.1002/jgrg.20087

Walter Anthony, K., Anthony, P., Grosse, G., & Chanton, J. (2012). Geologic methane seeps along boundaries of Arctic permafrost thaw and melting glaciers. *Nature Geoscience*, *5*, 419–426.

Walter Anthony, K., Daanen, R., Anthony, P., von Deimling, T. S., Ping, C.-L., Chanton, J. P., & Grosse, G. (2016). Methane emissions proportional to permafrost carbon thawed in Arctic lakes since the 1950s. *Nature Geoscience*, *9*, 679.

Walter Anthony, K., von Deimling, T. S., Nitze, I., Frolking, S., Emond, A., Daanen, R., et al. (2018). 21st-century modeled permafrost carbon emissions accelerated by abrupt thaw beneath lakes. *Nature Communications*, *9*(1), 3262. https://doi.org/10.1038/s41467-018-05738-9

Walter, K., Chanton, J., Chapin, F., Schuur, E., & Zimov, S. (2008). Methane production and bubble emissions from arctic lakes: Isotopic implications for source pathways and ages. *Journal of Geophysical Research*, *113*, G00A08. https://doi.org/10.1029/2007JG000569

Walter, K., Smith, L. C., & Chapin, F. S. (2007). Methane bubbling from northern lakes: Present and future contributions to the global methane budget. *Philosophical Transactions of the Royal Society A: Mathematical, Physical and Engineering Sciences*, *365*, 1657–1676.

Wang, D. T., Gruen, D. S., Lollar, B. S., Hinrichs, K. U., Stewart, L. C., Holden, J. F., et al. (2015). Nonequilibrium clumped isotope signals in microbial methane. *Science*, *348*(6233), 428–431. https://doi.org/10.1126/science.aaa4326

Wang, D. T., Welander, P. V., & Ono, S. (2016). Fractionation of the methane isotopologues $^{13}CH_4$, $^{12}CH_3D$, and $^{13}CH_3D$ during aerobic oxidation of methane by Methylococcus capsulatus (bath). *Geochimica et Cosmochimica Acta*, *192*, 186–202.

Whiticar, M. J. (1999). Carbon and hydrogen isotope systematics of bacterial formation and oxidation of methane. *Chemical Geology*, *161*, 291–314.

Wik, M., Crill, P. M., Varner, R. K., & Bastviken, D. (2013). Multiyear measurements of ebullitive methane flux from three subarctic lakes. *Journal of Geophysical Research: Biogeosciences*, *118*, 1307–1321. https://doi.org/10.1002/jgrg.20103

Wik, M., Thornton, B. F., Bastviken, D., MacIntyre, S., Varner, R. K., & Crill, P. M. (2014). Energy input is primary controller of methane bubbling in subarctic lakes. *Geophysical Research Letters*, *41*, 555–560. https://doi.org/10.1002/2013GL058510

Wik, M., Varner, R. K., Walter Anthony, K. M., MacIntyre, S., & Bastviken, D. (2016). Climate-sensitive northern lakes and ponds are critical components of methane release. *Nature Geoscience*, *9*, 99–105.

Winkel, M., Sepulveda-Jauregui, A., Martinez-Cruz, K., Heslop, J., Rijkers, R., Horn, F., et al. (2019). First evidence for cold-adapted anaerobic oxidation of methane in deep sediments of thermokarst lakes. *Environmental Research Communications*, *1*, 021002.

Young, E., Kohl, I. E., Lollar, B. S., Etiope, G., Rumble, D. III, Li, S., et al. (2017). The relative abundances of resolved CH_2D_2 and $^{13}CH_3D$ and mechanisms controlling isotopic bond ordering in abiotic and biotic methane gases. *Geochimica et Cosmochimica Acta*, *203*, 235–264. https://doi.org/10.1016/j.gca.2016.12.041

Yvon-Durocher, G., Allen, A. P., Bastviken, D., Conrad, R., Gudasz, C., St-Pierre, A., et al. (2014). Methane fluxes show consistent temperature dependence across microbial to ecosystem scales. *Nature*, *507*(7493), 488–491. https://doi.org/10.1038/nature13164